Journal of Nuclear Materials 526 (2019) 151754

Contents lists available at ScienceDirect

Journal of Nuclear Materials

journal homepage: www.elsevier.com/locate/jnucmat

Insights into the sources of irradiation hardening in a neutron irradiated 304L stainless steel following post-irradiation annealing

Z. Jiao*, J. Hesterberg, G.S. Was

Department of Nuclear Engineering and Radiological Sciences, University of Michigan, Ann Arbor, MI, USA

ARTICLE INFO

Article history:
Received 10 May 2019
Received in revised form
9 August 2019
Accepted 10 August 2019
Available online 13 August 2019

Keywords:
Irradiation hardening
Dislocation loops
Solute clusters
Post-irradiation annealing

ABSTRACT

The 304L SS was irradiated in Barsebäck 1 BWR reactor to 5.9 dpa followed by post-irradiation annealing at 500 °C and 550 °C up to 20 h. Correlations of irradiation hardening with the main hardening features of dislocation loops and Ni/Si-rich clusters were made using the least squares regression. The dispersed-barrier hardening model tended to overestimate the contribution of Ni/Si-rich clusters in the as-irradiated condition. Contribution of Ni/Si-rich clusters to irradiation hardening appeared to be more appropriately accounted for by the short-range order strengthening mechanism and was dependent on the Ni and Si concentrations in the clusters. Irradiation hardening in the as-irradiated condition was predominantly from dislocation loops with minor contribution from the Ni/Si-rich clusters. This is consistent with recent molecular dynamics simulations which showed that Ni/Si-rich clusters were weak obstacles to dislocation glide. As dislocation loops were annihilated at a faster pace than the Ni/Si-rich solute clusters, the Ni/Si-rich clusters played a more important role in the remaining hardening after thermal annealing. Contribution of Ni/Si-rich clusters to remaining hardening outweighed that of dislocation loops after thermal annealing at 550 °C for 5 h and became predominant after annealing for 20 h.

1. Introduction

Irradiation-assisted stress corrosion cracking (IASCC) is a major degradation mode of core stainless steel (SS) components in light water reactors. Many factors may contribute to IASCC [1,2] and yield strength is likely one of them. Studies [3,4] have shown that there is a correlation between yield strength and IASCC susceptibility with irradiation causing a substantial increase in yield strength (i.e. irradiation hardening), resulting in an increased susceptibility to IASCC. Irradiation hardening is caused by radiation-induced defects including dislocation loops, cavities, and radiation-induced solute clusters and second-phase particles.

The typical radiation-induced second phases in irradiated stainless steels include the γ′ (Ni_3Si) or G phase particles. The formation of these phases can be detected as extra diffraction spots corresponding to the γ′ or G phase in the diffraction mode of electron transmission microscopy (TEM), thus they can be revealed in the dark field images. On a finer scale, atom probe tomography (APT) provides a means of imaging radiation-induced Ni/Si-rich clusters that have yet to form a separate phase at low doses in both proton [5] and neutron irradiated stainless steels [6,7]. These Ni/Si-rich clusters have much lower Ni and Si concentrations than those in the γ′ or G phase. For the case of Ni/Si-rich clusters observed in 304L SS irradiated in boiling water reactor (BWR) to 5.9 dpa [6], the average Ni and Si concentrations were only 14 at% and ~3.0 at.%, respectively, well below that in the γ′ or G-phase. They are presumably precursors of the γ′ or G phase and may evolve to form these phases at higher doses.

Precipitation hardening from γ′ or G phase particles is expected to follow the typical dispersed-barrier hardening (DBH) model [8,9]. The hardening mechanism of Ni/Si-rich solute clusters in irradiated stainless steels is, however, not clear. The DBH model or its derivatives (such as the Bacon, Kocks, Scattergood (BKS) model [9]) have been used to model the contribution of solute clusters to hardening in irradiated stainless steels [7] and Fe-Cr alloys [10]. The DBH model assumes that the obstacles are hard particles which cause significant bowing of dislocations. This is unlikely for Ni/Si-rich clusters which have been shown to be weak obstacles and can be easily annihilated by dislocations [11,12]. Short-range order (SRO) strengthening has been successful in modeling the

* Corresponding author.
E-mail address: zjiao@umich.edu (Z. Jiao).

https://doi.org/10.1016/j.jnucmat.2019.151754
0022-3115/

contribution of Cu-Mg clusters in Al—Cu—Mg alloys [13] and is a more likely hardening mechanism for the Ni/Si-rich clusters in irradiated stainless steels.

Because post-irradiation annealing (PIA) partially removes dislocation loops and solute clusters by different degrees, multiple PIA conditions provide a unique opportunity to separate the contribution of solute clusters from dislocation loops in irradiation hardening using mathematical regression analysis. As the irradiation hardening and the microstructure data are recently available for a neutron irradiated 304L SS [6,14], a deeper understanding of the hardening mechanism of the Ni/Si-rich clusters can be gained.

2. Experiments

Neutron-irradiated 304L SS samples were prepared from a control rod that had reached 5.9 dpa by the end of service in the Barsebäck 1 BWR in Sweden. The irradiation temperature when the control rod was fully inserted was estimated to be ~288 °C. The chemical composition of the alloy in both weight percent and atomic percent is given in Table 1. PIA treatments were conducted at 500 °C for 1 h (500 °C:1h) and 550 °C for 1, 5 and 20 h (550 °C:1h, 550 °C:5h and 550 °C:20h) in an air furnace with accurate temperature control at the Oak Ridge National Laboratory. The annealing conditions were selected based on the degree of irradiation hardening and IASCC recovery [11]. The 500 °C:1h condition was sufficient to remove all IASCC susceptibility in four-point bend specimens while full mitigation of IASCC was observed for constant extension rate tensile test specimens at 550 °C:1h condition.

The main radiation-induced microstructure features in these samples were faulted dislocation loops and Ni/Si-rich clusters [6]. Al/Cu-rich clusters were also reported in the irradiated 304L SS in both the as-irradiated and post-irradiation annealed conditions. However, since the volume fraction of Al/Cu rich clusters (~0.035%) was only about 1% that of Ni/Si rich clusters (~2.5%) in the as-irradiated condition, its contribution to irradiation hardening was neglected. Irradiation hardening ($\Delta\sigma_y$), the increase in yield stress due to irradiation of the unirradiated 304L SS, is therefore caused mainly by radiation-induced dislocation loops and Ni/Si-rich clusters. Dislocation loops were characterized using the rel-rod dark field TEM technique and the Ni/Si-rich clusters were characterized using APT in the voltage operating mode. The detailed characterization results for dislocation loops and Ni/Si rich clusters were reported in Ref. [6] and the number densities, the average sizes, as well as the Ni and Si concentrations in the Ni/Si-rich clusters are given here in Table 2. The yield stress of irradiated 304L SS was determined from constant extension rate tensile (CERT) tests at 288 °C in simulated BWR water in the Irradiated Materials Testing Laboratory at the University of Michigan. Details on the CERT tests and the resulting irradiation hardening were reported in Ref. [14] and are also given here in Table 2.

3. Correlation results

Using the data provided in Table 2, a correlation of irradiated microstructure (dislocation loops and Ni/Si-rich clusters) with irradiation hardening can be made using both the DBH and SRO models for Ni/Si-rich clusters.

Table 1
Chemical compositions of the 304L SS control rod in the unirradiated state based on ladle analysis.

	C	Si	Mn	Cr	Co	N	Ni	P	S	Fe
wt%	0.025	0.30	1.09	18.35	0.029	0.024	10.57	0.013	0.003	Bal.
at%	0.11	0.59	1.09	19.45	0.03	0.09	9.92	0.02	0.005	68.68

3.1. Irradiation hardening using the DBH model for both dislocation loops and solute clusters

Based on the DBH model, the contribution of dislocation loops to irradiation hardening can be estimated using the following equation [8]:

$$\Delta\sigma_l = \alpha_l M \mu b \sqrt{N_l D_l} = \alpha_l f(N_l, D_l), \quad (1)$$

where, N_l is the dislocation loop number density and D_l is the average dislocation loop diameter; M is the Tylor factor of 3.06, μ the shear modulus of 76 GPa, and $\boldsymbol{b}$ is the Burgers vector of 0.255 nm; α_l is the strength factor (or hardening factor) for dislocation loops. Assuming that the DBH model also applies to the Ni/Si-rich clusters, the contribution of Ni/Si-rich clusters follows the same equation but substituting Ni/Si-rich clusters, denoted with α_c, for clusters, as shown in Eq. (2).

$$\Delta\sigma_c = \alpha_c M \mu b \sqrt{N_c D_c} = \alpha_c f(N_c, D_c), \quad (2)$$

When two or more obstacle barriers for dislocation glide are present, a superposition law must be chosen to account for the hardening contribution from each barrier. A power law for superposition may be assumed [15] as shown in Eq. (3) with k = 1 for linear-sum (LS) superposition and k = 2 for the root-sum-square (RSS) superposition. It is possible to find the most proper k value numerically based on dislocation dynamic simulations but it is out of the scope of this study.

$$(\Delta\sigma_y)^k = (\Delta\sigma_l)^k + (\Delta\sigma_c)^k \quad (3)$$

Although more complicated equation form for superposition may be used [16,17], the equation basically contains a RSS term and an LS term with a weighting supposition factor. In the case of neutron irradiated reactor pressure vessel steels or Fe-Cr alloys, the LS law is suggested for very different low ($\alpha < 0.05$) and high ($\alpha > 0.6$) obstacles while RSS law is suggested for obstacles with similar strength. The strength factors for dislocation loops may be dependent on the size of the dislocation loops [18] with typical values in the range of 0.25—0.5 [19]. In fact, Tan et al. [18] provided an empirical function, $\alpha = k_1 ln(k_2 d)$, to estimate the strength factor of dislocation loops by least-squares fitting of experimental data in neutron irradiated stainless steels. In their function, k_1 and k_2 are fitting parameters with values of 0.1969 and 1.4189, respectively, and d is the average diameter of dislocation loops. Using the empirical equation in Ref. [18], the strength factor for the as-irradiated condition is ~0.5, which yields irradiation hardening of ~900 MPa, nearly double the measured irradiation hardening of 474 MPa, and the strength factor for the 550 °C:20h condition is estimated to be ~0.7, which overestimates the irradiation hardening by ~20%. It appears that the empirical function does not correctly predict the irradiation hardening quantitatively in our case. In fact, the average dislocation loop diameters in all but the 550 °C:20h condition are similar with an average of 8.7 nm. Therefore, single strength factor for all of these conditions should be appropriate.

As the strength factor for the Ni/Si-rich clusters is unknown, the LS law was first tried using a least squares fit for the data in Table 2 which yielded $\alpha_c = 0.06 \pm 0.01$ and $\alpha_l = 0.15 \pm 0.03$. The strength factor for dislocation loops is much lower than the expected value (0.25—0.5) and the difference between α_c and α_l is not large enough as suggested for the LS law. The RSS law for supposition of hardening contribution from dislocation loops and Ni/Si-rich solute

Table 2
Characteristics of dislocation loops and Ni/Si-rich solute clusters [6] as well as the measured yield stress [14] in the neutron irradiated 304L in the as-irradiated and various thermal annealing conditions.

PIA Condition	Dislocation loops		Ni/Si-rich clusters				Measured $\Delta\sigma_y$ (MPa)
	Number density, N ($10^{22}m^{-3}$)	Avg. diameter, D (nm)	Number density, N ($10^{23}m^{-3}$)	Avg. diameter, D (nm)	% of Ni consumed by cluster	% of Si consumed by cluster	
As-Irradiated	11.1 ± 2.2	8.3 ± 1.0	3.9 ± 0.6	9.2 ± 0.7	17.7 ± 1.3	52.8 ± 1.7	474.0
500 °C:1h	8.2 ± 1.6	9.6 ± 1.0	2.8 ± 0.5	10.8 ± 0.9	17.8 ± 4.0	52.7 ± 8.4	421.9
550 °C:1h	3.3 ± 0.7	8.9 ± 1.0	2.4 ± 0.1	12.3 ± 1.0	23.6 ± 0.2	56.4 ± 0.4	341.7
550 °C:5h	1.3 ± 0.3	8.0 ± 1.0	1.2 ± 0.5	18.1 ± 4.7	29.9 ± 0.0	56.4 ± 0.0	272.2
550 °C:20h	0.05 ± 0.01	26 ± 4	0.7 ± 0.1	20.2 ± 1.4	24.5 ± 0.6	43.0 ± 0.5	125.4

clusters appears to be a better choice than the LS law.

Following the RSS superposition law for dislocation loops and Ni/Si-rich solute clusters, the total contribution of dislocation loops and Ni/Si-rich clusters to the increase in the yield strength is:

$$(\Delta\sigma_y)^2 = (\Delta\sigma_l)^2 + (\Delta\sigma_c)^2 = [\alpha_l f(N_l, D_l)]^2 + [\alpha_c f(N_c, D_c)]^2. \quad (4)$$

Using the data provided in Table 2 for irradiation hardening ($\Delta\sigma_y$), dislocation loops number density and size (N_l, D_l), and Ni/Si-rich cluster parameters (N_c, D_c), α_l and α_c can be obtained by a least squares fit to Eq. (2). The fitting results are given in Table 3 and yield $\alpha_l = 0.20 \pm 0.01$ and $\alpha_c = 0.08 \pm 0.01$. The fitting strength factor for dislocation loops without the 550 °C:20h condition is 0.19 ± 0.01, which is within the error of that (0.20 ± 0.01) obtained including the 550 °C:20h condition. Therefore, the strength factor for the 550 °C:20h condition does not vary significantly from other conditions and this condition is included in the regression analysis. Using the fitted strength factors for dislocation loops and the Ni/Si-rich clusters, the resulting irradiation hardening from dislocation loops ($\Delta\sigma_l$), Ni/Si-rich clusters ($\Delta\sigma_c$) as well as the total contribution from both are given in Table 4 and compared with the measured irradiation hardening data in Fig. 1a. The contribution of solute clusters to hardening is slightly lower than that of dislocation loops in both the as-irradiated and 500 °C:1h conditions while the situation is reversed at PIA conditions beyond 550 °C:1h. As another measure of the contribution of dislocation loops and Ni/Si-rich clusters to the total irradiation hardening, the ratios of hardening solely from dislocations loops or Ni/Si-rich clusters to the total irradiation hardening are given in Table 4 and the evolution of the ratios with PIA is shown in Fig. 2. It can be clearly seen that the fraction of contribution from dislocation loops to the total remaining hardening decreases with extent of thermal annealing and becomes insignificant at 550 °C:20h when loops have mostly disappeared.

3.2. Irradiation hardening using SRO strengthening model for solute clusters

Starink and Wang [13] have shown that short-range ordering is the main strengthening mechanism for Cu-Mg clusters in Al alloys due to the change in energy related to the short-range order per unit area on slip planes in the clusters relative to that in the matrix. In other words, dislocations must break a different number of Ni-Si bonds in the Ni/Si-rich clusters than in the matrix which requires energy, thus causing strengthening. It is obvious that the degree of strengthening should depend on the Ni and Si concentration in the clusters. Following Starink and Wang's analysis for Cu-Mg clusters in FCC Al alloys, the contribution of short-range order strengthening takes the following form for Ni/Si-rich clusters in the 304L SS with the same FCC crystal structure:

$$\Delta\sigma_c = M\Delta\tau_{SRO} \cong M\frac{\Delta H_{Ni-Si}}{b^3} \times \frac{4}{\sqrt{3}}\left[\frac{2}{3}(y_{Ni}+y_{Si}) - \left(\frac{2}{3}y_{Ni}x_{si} + \frac{2}{3}y_{Si}x_{Ni} + 2x_{Ni}x_{Si}\right)\right] = \Delta H_{Ni-Si} f(y_{Ni}, y_{Si}, x_{Ni}, x_{Si}), \quad (5)$$

Where ΔH_{Ni-Si} is the mixing enthalpy of Ni-Si bond in the Ni/Si-rich clusters, y_{Ni} is the amount of Ni atoms in the Ni/Si-rich clusters, and y_{Si} is the amount of Si atoms in the clusters. The amount of Ni atoms in the matrix phase is x_{Ni} and the amount of Si atoms in the matrix phase is x_{Si}. As the atom probe tomography analysis has provided Ni and Si composition information in the Ni/Si-rich clusters (Table 2), $f(y_{Ni}, y_{Si}, x_{Ni}, x_{Si})$ in Eq. (3), which is dependent on the cluster and matrix composition at all examined conditions can be determined and the values are given in Table 5. Note that the contribution of Ni/Si-rich clusters to hardening is dependent on ΔH_{Ni-Si}, which is not known. However, it can be obtained indirectly by least-square fitting of Eq. (4), similar to the process used to obtain the strength factor for solute clusters:

$$(\Delta\sigma_y)^2 = (\Delta\sigma_l)^2 + (\Delta\sigma_c)^2 = [\alpha_l f(N_l, D_l)]^2 + [\Delta H_{Ni-Si} f(y_{Ni}, y_{Si}, x_{Ni}, x_{Si})]^2, \quad (6)$$

Through a least squares fit to Eq. (4), both α_l and ΔH_{Ni-Si} can be obtained. The fitting results are given in Table 3. The strength factor for dislocation loops, α_l, is determined to be 0.25 ± 0.01 and the value of ΔH_{Ni-Si} is estimated to be ~14 kJ/mol. Using the fitted values for α_l and ΔH_{Ni-Si}, contributions of dislocation loops and solute clusters to hardening at the as-irradiated and various PIA conditions are given in Table 4 and the comparison is made in Fig. 1b. Contribution of dislocation loops to hardening is dominant in both the as-irradiated and 500 °C:1h conditions while contribution of Ni/Si rich clusters to hardening becomes dominant after thermal annealing at 550 °C for 5 h.

Table 3
Strength factors for dislocation loops (α_l) and Ni/Si-rich clusters (α_c)or Ni-Si mixing enthalpy ($\Delta H_{Ni\text{-}Si}$) obtained by least squares regression fitting for different hardening models.

DBH for dislocation loops DBH for Ni/Si-rich clusters		DBH for dislocation loops SRO for Ni/Si-rich clusters	
α_l - DBH	α_c - DBH	α_l - DBH	$\Delta H_{Ni\text{-}Si}$ -SRO
0.20 ± 0.01	0.08 ± 0.01	0.25 ± 0.01	14 ± 2 (KJ/mol)

Table 4
Contribution to irradiation hardening by dislocation loops and Ni/Si-rich solute clusters by different hardening models.

Thermal annealing condition	DBH for dislocation loops and Ni/Si-rich clusters					DBH for dislocation loops, SRO for Ni/Si-rich clusters					Measured $\Delta\sigma_y$ (MPa)
	$\Delta\sigma_l$ (MPa)	$\Delta\sigma_c$ (MPa)	$\Delta\sigma_y$ (MPa)	$\Delta\sigma_l/\Delta\sigma_y$	$\Delta\sigma_c/\Delta\sigma_y$	$\Delta\sigma_l$ (MPa)	$\Delta\sigma_c$ (MPa)	$\Delta\sigma_y$ (MPa)	$\Delta\sigma_l/\Delta\sigma_y$	$\Delta\sigma_c/\Delta\sigma_y$	
As-Irradiated	360 ± 36	284 ± 36	459 ± 64	0.79	0.62	450 ± 18	133 ± 19	469 ± 70	0.96	0.28	474.0
500 °C:1h	333 ± 33	262 ± 33	424 ± 59	0.79	0.62	416 ± 17	134 ± 19	437 ± 66	0.95	0.31	421.9
550 °C:1h	202 ± 20	255 ± 32	325 ± 46	0.62	0.78	252 ± 10	175 ± 25	307 ± 46	0.82	0.57	341.7
550 °C:5h	120 ± 12	222 ± 28	252 ± 35	0.47	0.88	149 ± 6	217 ± 31	264 ± 40	0.57	0.82	272.2
550 °C:20h	43 ± 4	178 ± 22	183 ± 26	0.23	0.97	53 ± 2	175 ± 25	183 ± 27	0.29	0.96	125.4

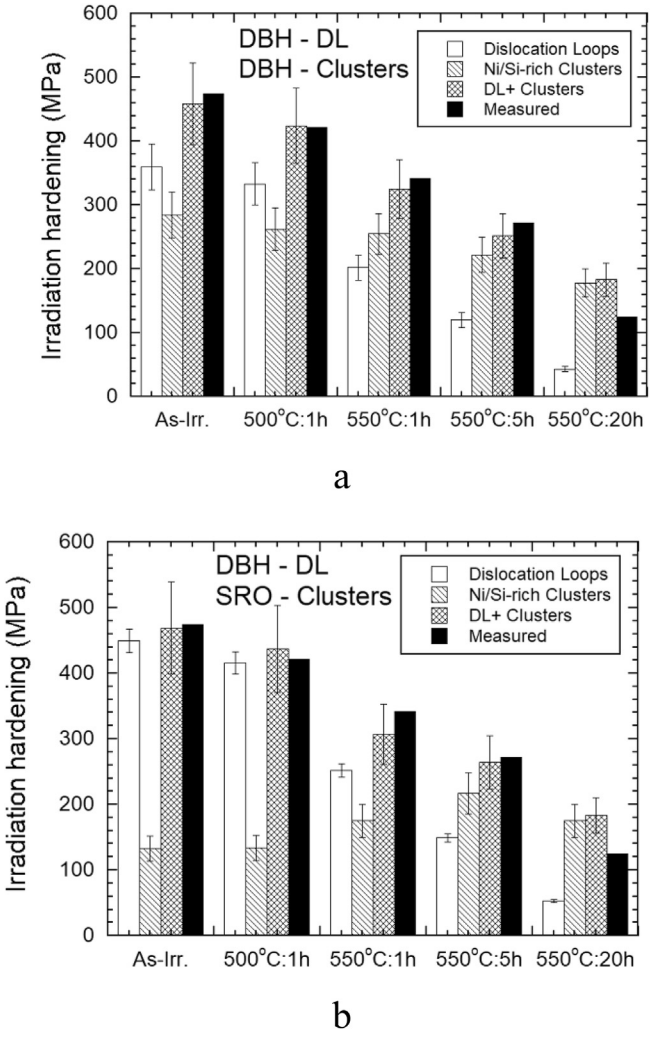

Fig. 1. Comparison of contribution to irradiation hardening calculated from different hardening models: (a) DBH for dislocation loops and Ni/Si-rich clusters (b) DBH for dislocation loops and SRO for Ni/Si-rich clusters in neutron irradiated 304L SS to 5.9 dpa in the as-irradiated and various thermal annealing conditions.

4. Discussion

For the convenience of discussion, the "DBH model" refers to the case where the DBH model is used for both dislocation loops and Ni/Si-rich clusters while the "SRO model" refers to the case where DBH is used for dislocation loops but SRO model is used for Ni/Si-rich clusters. Both DBH and SRO models show a similar trend on the thermal annealing effect on the contribution fraction of hardening by dislocation loops and Ni/Si-rich clusters in irradiated 304L SS. The normalized fractional contribution to the total irradiation hardening decreases with thermal annealing for dislocation loops

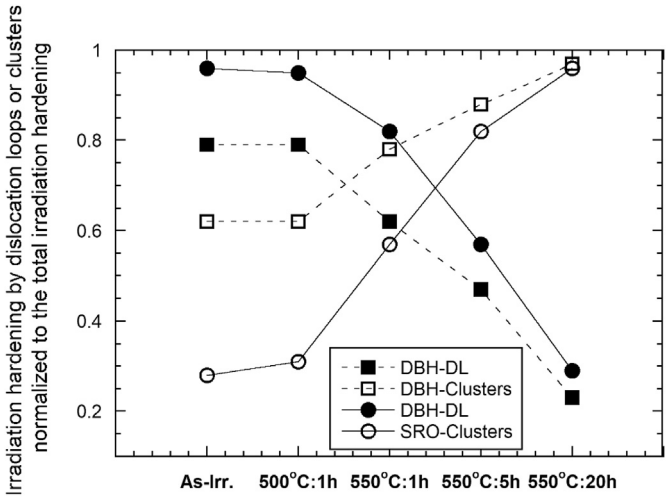

Fig. 2. Contribution of dislocation loops and Ni/Si-rich clusters, as calculated using the DBH or SRO model for clusters, to irradiation hardening in neutron irradiated 304L SS to 5.9 dpa in the as-irradiated state and after various thermal annealing conditions.

but increases for Ni/Si-rich clusters (Fig. 2). At 550 °C:5h, the contribution of Ni/Si-rich is dominant for remaining irradiation hardening for both DBH and SRO models. This is mainly due to the fact that dislocation loops are annihilated at a faster pace than Ni/Si-rich clusters. The major difference between these two models is the absolute value in contribution of dislocation loops and solute clusters, particularly in the as-irradiated condition. Although both models show a higher contribution from dislocation loops, the contribution of Ni/Si-rich clusters is quite different. As shown in Table 4, dislocation loops alone would account for 79% of total irradiation hardening for DBH model and 96% for the SRO model in the as-irradiated condition. Ni/Si-rich clusters alone would account for 62% irradiation hardening for DBH model and 28% for the SRO model in the as-irradiated condition. Note that the contribution percentage does not add up to 100% because of the RSS superposition rule. To put this in a way that can be easily understood, if there is an alloy A which only has dislocation loops with the same size and number density as those in the irradiated 304L SS, the irradiation hardening in alloy A would be 96% of that in 304L SS according the SRO model, even though no Ni/Si-rich clusters exist in alloy A. Similarly, if there is an alloy B which only has the Ni/Si-rich clusters with the same size and number density as those in the irradiate 304L SS, the irradiation hardening in alloy B would be 28% of that in 304L SS according to the SRO model. Although Ni/Si-rich clusters do contribute to irradiation hardening, the contribution in the context of high density of dislocation loops in the as-irradiation condition is minor according to the SRO model. The DBH model shows a much more significant contribution of Ni/Si-rich clusters in the as-irradiated conditions. So the question is which model yields a more accurate prediction of the contribution of Ni/Si-rich clusters to irradiation hardening?

Table 5
Ni and Si concentration characteristics of Ni/Si-rich clusters based on the % of Ni and Si consumed by the clusters as shown in Table 2. $f(y_{Ni}, y_{Si}, x_{Ni}, x_{Si})$ is as defined in Eq. (5).

Thermal annealing condition	Ni atoms in Ni-Si clusters y_{Ni} (%)	Ni atoms in matrix x_{Ni} (%)	Si atoms in Ni-Si clusters y_{Si} (%)	Si atoms in matrix x_{Si} (%)	$f(y_{Ni}, y_{Si}, x_{Ni}, x_{Si})$
As-Irradiated	1.76	8.16	0.31	0.28	9.51
500 °C:1h	1.77	8.15	0.31	0.28	9.56
550 °C:1h	2.34	7.58	0.33	0.26	12.49
550 °C:5h	2.97	6.95	0.33	0.26	15.53
550 °C:20h	2.43	7.49	0.25	0.34	12.47

The DBH model has worked reasonably well for dislocation loops which are relative strong obstacles to dislocation glide. The strength factors of 0.20 for DBH and 0.25 for SRO are both reasonable for dislocation loops. The DBH model yields a strength factor of 0.08 for Ni/Si-rich clusters. This is comparable to that of neutron irradiated 304 SS at 300 °C to 24 dpa which has a suggested strength factor of 0.11 [7]. However, the average Ni and Si concentrations in the Ni/Si-rich clusters observed in the 304 SS at 24 dpa were 40% and 14%, respectively, which are much higher than those observed in the 304L SS in this study which has 14.3 at% of Ni and 3 at% of Si in the as-irradiated condition [6]. As the γ′ (75% Ni, 25% Si) has a suggested strength factor of 0.4 [20–22], the strength factor is apparently dependent on the concentrations of Ni and Si in the clusters or precipitates. This is consistent with the SRO model in which hardening is dependent on the amount of Ni-Si bonds in the clusters. The Ni and Si concentrations in the Ni/Si-rich clusters in 304L SS at 5.9 dpa is about 1/3-1/5 of those in 304 SS at 24 dpa. A strength factor of 0.02–0.04 appears to be more reasonable for the Ni/Si-rich clusters in 304L SS at 5.9 dpa. This is also consistent with the predication of molecular dynamic simulation which suggests a strength factor of 0.03 [11] for Ni/Si-rich clusters in 304L SS with the characterized average Ni and Si concentrations. The strength factor of 0.08 for Ni/Si-rich clusters from DBH model and correlation appears to be too big and would overestimate the contribution of Ni/Si-rich clusters to irradiation hardening in irradiated 304L SS in this study. It appears that the DBH model may be still used but the strength factor needs to be scaled properly based on the Ni and Si concentration in the clusters.

The literature data also suggests that the contribution of Ni/Si-rich clusters is less significant than that of dislocation loops in the as-irradiated conditions. For instance, the difference in irradiation hardening (ΔHv) for austenitic steels with (alloy H) and without (alloy E) Ni/Si-rich clusters is minimal (193 kg/mm^2 for alloy H vs. 188 kg/mm^2 for alloy E) after proton irradiation at 360 °C for 5.5 dpa [23]. Irradiation hardening from neutron irradiation also shows minimal difference for alloy H (248 kg/mm^2, BOR60, 7.8 dpa) and alloy E (233 kg/mm^2, BOR60, ~10 dpa) [23]. Both proton and neutron irradiation show that alloy E has >90% of irradiation hardening of alloy H, indicating that the Ni/Si-rich clusters play a minor role in irradiation hardening in the as-irradiated conditions. This is again consistent with the result from SRO model. The hardening mechanism of Ni/Si-rich clusters with low Ni and Si concentration is therefore due to the breaking of existing Ni-Si bonds rather than dislocation bowing around the clusters, which is supported by the molecular dynamics simulations [11]. This, however, only applies to Ni/Si-clusters that are formed at relatively low irradiation doses. The γ′ or G phase particles that are formed at high doses are expected to be strong barriers and the DBH model should be appropriate.

5. Conclusions

The contribution of Ni/Si-rich solute clusters to irradiation hardening has been evaluated based on DBH and SRO models in neutron irradiated 304L SS irradiated in the BWR to 5.9 dpa after thermal annealing at different conditions.

- The irradiation hardening of Ni/Si-rich solute clusters can be better predicted using the SRO strengthening model than the DBH model, which tends to overestimates the contribution of Ni/Si clusters to irradiation hardening in the as-irradiated condition.
- Dislocation loops dominate the irradiation hardening in the as-irradiated condition. Ni/Si-rich clusters contribute to irradiation hardening but play a minor role in the as-irradiated condition. This is consistent with observations in literature for irradiated stainless steels.
- Ni/Si-rich clusters dominate the irradiation hardening after thermal annealing at 550 °C to 5 h.
- The strength factor for dislocation loops is determined to be ~0.25 and the fitting parameter for Ni-Si mixing enthalpy is determined to be ~14 kJ/mol based on the SRO model and least squares regression of the as-irradiated and thermal annealed 304L SS.

Acknowledgements

The authors acknowledge the characterization facilities at ORNL-LAMBA and the Michigan Center for Materials Characterization at University of Michigan for microstructure characterization work. Support for this research was provided by Department of Energy under contract number DE-AC07-05ID14517.

References

[1] G. Was, P. Andresen, Corrosion 63 (2007) 19–45.
[2] Z. Jiao, G.S. Was, J. Nucl. Mater. 408 (2011) 246.
[3] S.M. Bruemmer, E.P. Simonen, P.M. Scott, P.L. Andresen, G.S. Was, J.L. Nelson, J. Nucl. Mater. 274 (1999) 299–314.
[4] M.O. Speidel, R. Magdowski, in: F.P. Ford, S.M. Bruemmer, G.S. Was (Eds.), Ninth International Symposium on Environmental Degradation of Materials in Nuclear Power Systems — Water Reactors, Metallurgical Society of AIME, Warrendale, PA, 1999, pp. 325–329.
[5] Z. Jiao, G.S. Was, Acta Mater. 59 (2011) 1220–1238.
[6] Z. Jiao, J. Hesterberg, G.S. Was, J. Nucl. Mater. 500 (2018) 220–234.
[7] T. Toyama, Y. Nozawa, W. Van Renterghem, Y. Matsukawa, M. Hatakeyama, Y. Nagai, A. Al Mazouzi, S. Van Dyck, J. Nucl. Mater. 418 (2011) 62–68.
[8] A.K. Seeger, On the theory of radiation damage and radiation hardening, in: Proceedings of the Second United Nations International Conference on the Peaceful Uses of Atomic Energy, vol. 6, United Nations, New York, September 1958, pp. 250–273. Geneva.
[9] D.J. Bacon, U.F. Kocks, R.O. Scattergood, Philos. Mag. 28 (1973) 1241–1263.
[10] F. Bergner, C. Pareige, M. Hernández-Mayoral, L. Malerba, C. Heintze, J. Nucl. Mater. 448 (2014) 96–102.
[11] Justin Hesterberg, Richard Smith, Gary S Was, Atomistic simulation of the obstacle strengths of radiation-induced defects in an Fe-Ni-Cr austenitic stainless steel, Model. Simul. Mater. Sci. Eng.
[12] Z. Jiao, M. McMurtrey, G.S. Was, Scr. Mater. 65 (2011) 159–163.
[13] M.J. Starink, S.C. Wang, Acta Mater. 57 (2009) 2376–2389.
[14] J. Hesterberg, Z. Jiao, G.S. Was, Effects of post-irradiation annealing on the IASCC susceptibility of neutron-irradiated 304L stainless steel, J. Nucl. Mater. (2018).
[15] J.-S. Wang, M.D. Mulholland, G.B. Olson, D.N. Seidman, Acta Mater. 61 (2013) 4939–4952.
[16] G.R. Odette, G.E. Lucas, Radiat. Eff. Defect Solid 144 (1–4) (1998) 189–231.

[17] Dhriti Bhattacharyya, Takuya Yamamoto, Peter Wells, Emmanuelle Marquis, Mukesh Bachhav, Yuan Wu, Joel Davis, G. Alan Xu, Robert Odette, J. Nucl. Mater. 519 (2019) 274–286.
[18] L. Tan, J.T. Busby, J. Nucl. Mater. 465 (2015) 724–730.
[19] G.S. Was, Fundamentals of Radiation Materials Science, second ed., Springer-Verlag, Berlin, 2017.
[20] G.E. Lucas, J. Nucl. Mater. 206 (1993) 287–305.
[21] B.H. Sencer, J. Nucl. Mater. 345 (2005) 136–145.
[22] K. Fukuya, K. Fujii, H. Nishioka, Y. Kitsunai, J. Nucl. Sci. Technol. 43 (2006) 159–173.
[23] K.J. Stephenson, G.S. Was, J. Nucl. Mater. 456 (2015) 85–98.